科学通报 2017 年 第 62 卷 第 2-3 期：107 ~ 121
专题：自驱动微马达 评 述
《中国科学》杂志社
SCIENCE CHINA PRESS

自驱动微纳米马达的设计原理与结构简化方法

孔磊, 牟方志, 姜玉周, 李小丰, 官建国*

武汉理工大学材料科学与工程国际化示范学院, 材料复合新技术国家重点实验室, 武汉 430070
* 联系人, E-mail: guanjg@whut.edu.cn

2016-07-29 收稿, 2016-09-08 修回, 2016-09-12 接受, 2016-10-17 网络版发表
国家自然科学基金(51303144, 21474078, 51521001)、湖北省高端人才引领培养计划、湖北省自然科学基金创新群体项目(2015CFA003)和中央高校基本科研业务费专项(WUT: 2015III060, 2016III009)资助

摘要 自驱动微纳米马达由于其自主运动特性, 在药物运输、生物传感、细胞分离、微手术和环境治理等方面有着重要的应用前景. 本文通过分析自驱动微纳米马达的气泡反冲和自泳等各种驱动机理, 指出设计制备自驱动微纳米马达的关键是在微纳米粒子周围构建非对称场; 重点综述了自驱动微纳米马达从双面神结构和多层管状结构到各向异性单组分结构和各向同性粒子的结构演变与简化历程, 并对其发展和应用前景做出了展望.

关键词 微纳米马达, 自驱动, 非对称场, 结构简化

自驱动微纳米马达(micro-/nanomotors, MNMs)是一种能够将其他形式的能量转化为动能产生自主运动的微纳米器件. 由于微纳米马达具有独特的运动特性, 可在液相介质中装载、运输和释放各种微纳米货物, 因此在药物运输、生物传感、细胞分离、微手术和环境治理等方面有着很多引人注目的应用前景[1~8]. 自驱动微纳米马达的驱动机理可以分为气泡反冲驱动机理和自泳驱动机理[9]. 其中, 气泡反冲驱动机理是基于气泡在脱离马达的瞬间形成的连续动量变化导致了马达的持续运动[10], 自泳驱动机理是指产物或热量非对称地释放在马达周边形成了局部电场、浓度梯度、表面张力梯度和温度梯度等导致马达的运动[11]. 这些驱动机理的本质在于构建一个非对称场, 通过非对称场来打破马达的静力平衡, 使微纳米马达产生运动. 在过去的近20年里, 人们对于非对称场的构建进行了大量的研究[12,13]. 最早, 采用双面神结构的粒子、双金属管或棒, 通过惰性层或反应活性层的非对称修饰实现了非对称场的建立. 同时, 也可以采用多层管状结构使惰性层处在管最外侧屏蔽外层的反应, 活性层处在管内侧, 在管内外形成了非对称场. 后来, 直接使用各向异性单组分粒子、管状或罐状结构, 不需要惰性层的修饰, 通过形状的不规则性、气泡在凹凸表面成核的难易程度形成了非对称场[14]. 最近, 采用各向同性的粒子, 通过特殊的外场刺激, 可以直接在粒子的两侧产生非对称的化学反应形成非对称场. 目前, 已有多篇外文综述[7,12,13,15~19]对微纳米马达的驱动机理、制备方法和应用做出了总结, 但是对自驱动微纳米马达的本质以及围绕该本质如何构建微纳米马达并没有阐述. 本文主要介绍自驱动微纳米马达的驱动机理, 包括气泡反冲驱动和自泳驱动, 并指出设计制备自驱动微纳米马达的关键是在微纳米粒子周围构建非对称场. 针对非对称场的构建策略, 重点评述微纳米马达从双面神结构和多层管状结构演变为各向异性单组分结构和各向同性粒子的动态过程, 及其制备方法和结构的逐步简化以及运动的可控性.

引用格式: 孔磊, 牟方志, 姜玉周, 等. 自驱动微纳米马达的设计原理与结构简化方法. 科学通报, 2017, 62: 107–121
Kong L, Mou F Z, Jiang Y Z, et al. Design strategies and structure simplification methods of self-propelled micro-/nanomotors (in Chinese). Chin Sci Bull, 2017, 62: 107–121, doi: 10.1360/N972016-00841

1 自驱动微纳米马达的驱动机理

自驱动微纳米马达的驱动机理包括气泡反冲驱动机理和自泳驱动机理. 气泡反冲驱动机理由Whitesides课题组[20]在2002年提出, 是最早出现的一种驱动方式. 之后通过理论计算和实验验证[10,21,22]发现, 气泡型微纳米马达的动力来源是气泡在脱离马达的瞬间形成的连续动量变化导致了马达的持续运动(图1(a)). 由于气泡驱动型的微纳米马达具有驱动力大等优势[29], 因此在较长的时间内都是研究热点. 自泳驱动是比较特殊的一类驱动方式, 通过产物或热量的非对称释放在马达周边形成了局部电场、浓度梯度、表面张力梯度和温度梯度等, 从而导致马达的运动. 离子型产物的释放通常会在马达周边形成局部电场, 使带电粒子在自建电场中运动或是产生相互聚集和排斥行为, 即马达的自电泳或自扩散电泳

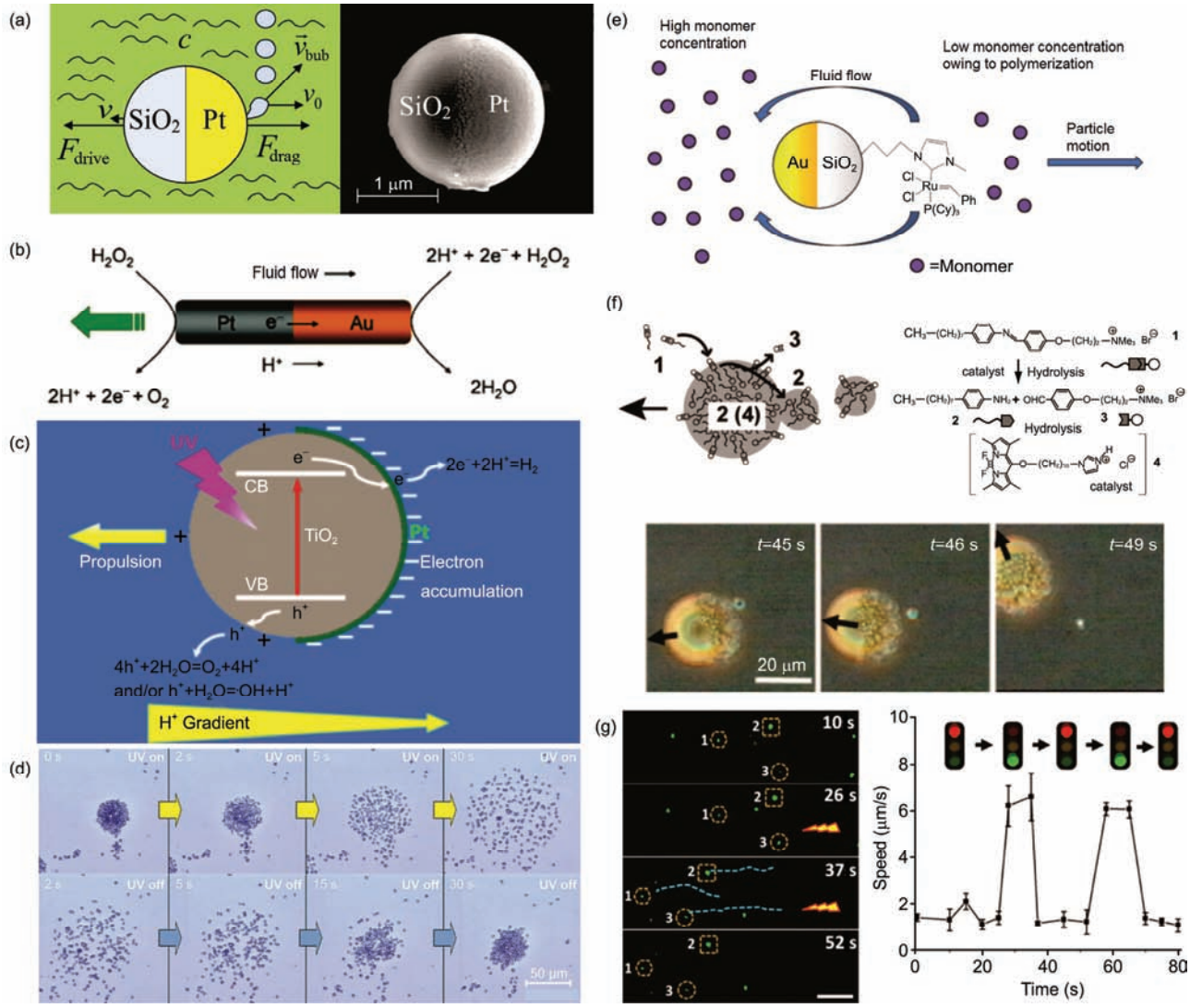

图 1 (网络版彩色)(a) 通过气泡反冲驱动的SiO_2/Pt双面神粒子[10]; (b) 自电泳驱动的Pt-Au马达[23]; (c) TiO_2/Pt亚微米马达在纯水中的运动机理[24]; (d) SiO_2-TiO_2双面神粒子在紫外光控制下的聚集和排开[25]; (e) Grubbs催化剂修饰的Au/SiO_2马达基于自扩散泳的运动[26]; (f) 通过消耗表面活性剂自驱动的油滴[27]; (g) 金纳米粒子修饰的多孔二氧化硅双面神纳米马达在自热泳驱动下的运动[28]

Figure 1 (Color online) (a) The movement of SiO_2/Pt Janus particle by bubble propulsion[10]. (b) Self-electrophoresis movement of Pt-Au nanosubmarine[23]. (c) Schematic diagram of the propulsion mechanism of the water-fuelled TiO_2/Pt submicromotor[24]. (d) The schooling and exclusion motion behaviors of SiO_2-TiO_2 Janus particles in deionized water controlled by UV irradiation[25]. (e) The Grubbs' catalyst modified Au/SiO_2 micromotors moving by self-diffusiophoresis[26]. (f) Representative illustration of a self-propelled oil droplet consuming "fuel" surfactant[27]. (g) The movement of AuNS-modified Janus mesoporous silica nanoparticle motors by self-thermophoresis[28]

驱动机理[18,30]. Mallouk课题组[23,31,32]在Pt-Au双金属棒马达体系中将双氧水浓度降到很低时，发现马达会指向Pt一端运动. 他们认为Pt和Au形成了原电池结构，在Pt的一端发生了氧化反应失去电子，电子迁移到Au一端发生还原反应. 质子会在Pt的一端形成高浓度区，在Au的一端形成低浓度区，这样就形成了局部电场，带负电的双金属棒会在这样的电场中指向Pt端运动，这就是自电泳(图1(b)). 最近，本课题组[24]和任碧野课题组[33]分别将光催化材料TiO_2与贵金属Pt和Au复合形成双面神粒子，该粒子在紫外光照射下基于自电泳机理能够在纯水中快速运动(图1(c)). 由于阴阳离子的扩散速率不同，在粒子周边会形成放射状的局部电场，通常应用于微纳米泵[18]. Sen课题组[25]研究了SiO_2-TiO_2双面神微米粒子在紫外光控制下的聚集和散开过程，认为TiO_2在光照下产生了$\cdot O_2^-$，·OH和H^+等物质，在扩散时形成了局部电场，带电粒子会沿着电场方向运动(图1(d)). AgCl粒子也有同样的效果，在紫外光照下像“烟花”一样的散开-聚集[34]. 非离子型产物则会形成较大的浓度梯度，在渗透压作用下形成由低浓度区向高浓度区的流体流动，从而使粒子产生自扩散泳运动. Sen课题组[26]制备了Au-SiO_2双面神粒子，然后在二氧化硅表面修饰Grubb催化剂，马达在含有降冰片烯单体的溶液中能够引发单体的开环易位聚合，此时二氧化硅一侧的单体浓度会急剧下降，流体会向着单体浓度高的一侧流动，推动马达朝着二氧化硅端运动(图1(e)). 产物的非对称释放除了会形成局部电场和浓度梯度外还会形成表面张力梯度，从而在马朗格尼效应作用下驱动马达的运动[35]. 基于马朗格尼效应运动的马达具有运动速度快的特点，而且一些宏观的物体也能够快速运动. Sugawara课题组[27]开发了一种利用催化分解表面活性剂而自主运动的油滴，油滴中含有能够催化分解水相中表面活性剂的催化剂，在油滴表面的表面活性剂不断被分解，于是在油滴的周围形成了表面张力梯度推动油滴运动(图1(f)). 此外，液滴通过马朗格尼效应也能在一些改性后的基板上运动[36~38]，一些低极性的樟脑分子、乙醇分子和二甲基甲酰胺(DMF)分子等在水中非对称的释放也能产生表面张力梯度引起运动[39~43]. 在光照作用下，一些微纳米马达的周围也会形成温度梯度，从而产生自热泳，推动马达的运动. 贺强课题组[28,44]采用金纳米粒子非对称修饰的多孔二氧化硅纳米粒子在近红外光作用下，能够在其周边形成较大的温度梯度，产生自热泳驱动运动(图1(g)).

总之，无论是气泡反冲驱动还是自泳驱动的微纳米马达，都要在其周围形成一个非对称场，打破马达的静力平衡从而产生自主运动. 在过去的近20年里，人们对于如何建立这样一个非对称场进行了大量的研究探讨. 起初大多采用表面非对称改性、电化学沉积的方法制备一些非对称的双面神结构和利用模板辅助法、薄膜自卷曲法得到一些多层管状结构来构建微纳米马达；后来又发展了各向异性单组分粒子、管状或罐状结构的微纳米马达. 最近，又实现了各向同性粒子的运动. 下文将按此线索详细评述不同结构的微纳米马达的制备方法、运动特性和独特的应用性能.

2 双面神结构马达

双面神结构粒子(Janus particles)是指2个半球表面具有不同物理化学性质的各向异性粒子. 具有该结构的微纳米球、管或棒因为两面具有不同的物理化学性质，易于形成非对称场，从而产生运动. Mallouk课题组[45]采用电化学沉积的方法制备了Au-Pt双金属棒(图2(a))，通过双氧水在铂金两端不同的反应，实现了马达的运动[23]. Pt-Cu, Au-Ni, Rh-Au, Pd-Au, Ag-Cu等双金属马达也能够采用电化学沉积的方法很容易得到[32,50~53]. 后来，Golestanian课题组[54,55]先后通过模拟和实验的方法首次实现了双面神球形马达的运动. 本课题组[46]采用表面非对称改性的方法，先将微米镁球陷入PVP模板中，然后将Pt纳米粒子覆在裸露的镁球表面，最后将粒子从基板上超声剥离下来，通过扫描电子显微镜图片可以很清楚地看到双面神结构. 放入模拟体液(SBF)中，基于镁水反应产生氢气推动马达运动，从运动视频中可以看到反应只在马达的一侧发生(图2(b)). 采用类似的方法，聚苯乙烯微球、二氧化硅微球、铝及其合金微球等都可以制备成双面神结构[56~60]. Ozin课题组[47]将部分覆盖Pt的二氧化硅微球在高温下煅烧，Pt纳米粒子会经历熔融再结晶的过程. 由于Pt与二氧化硅之间较高的界面张力，Pt重结晶后会变成球形，最终形成葫芦状的SiO_2-Pt二聚体微米马达(图2(c)). Fischer课题组[61]采用斜角沉积的方法，制备了30 nm的Au-Pt双面神马达. Loget等人[48]利用两极电化学原理，当施加电场足够大、导电粒子的极化足够强时，电化学反

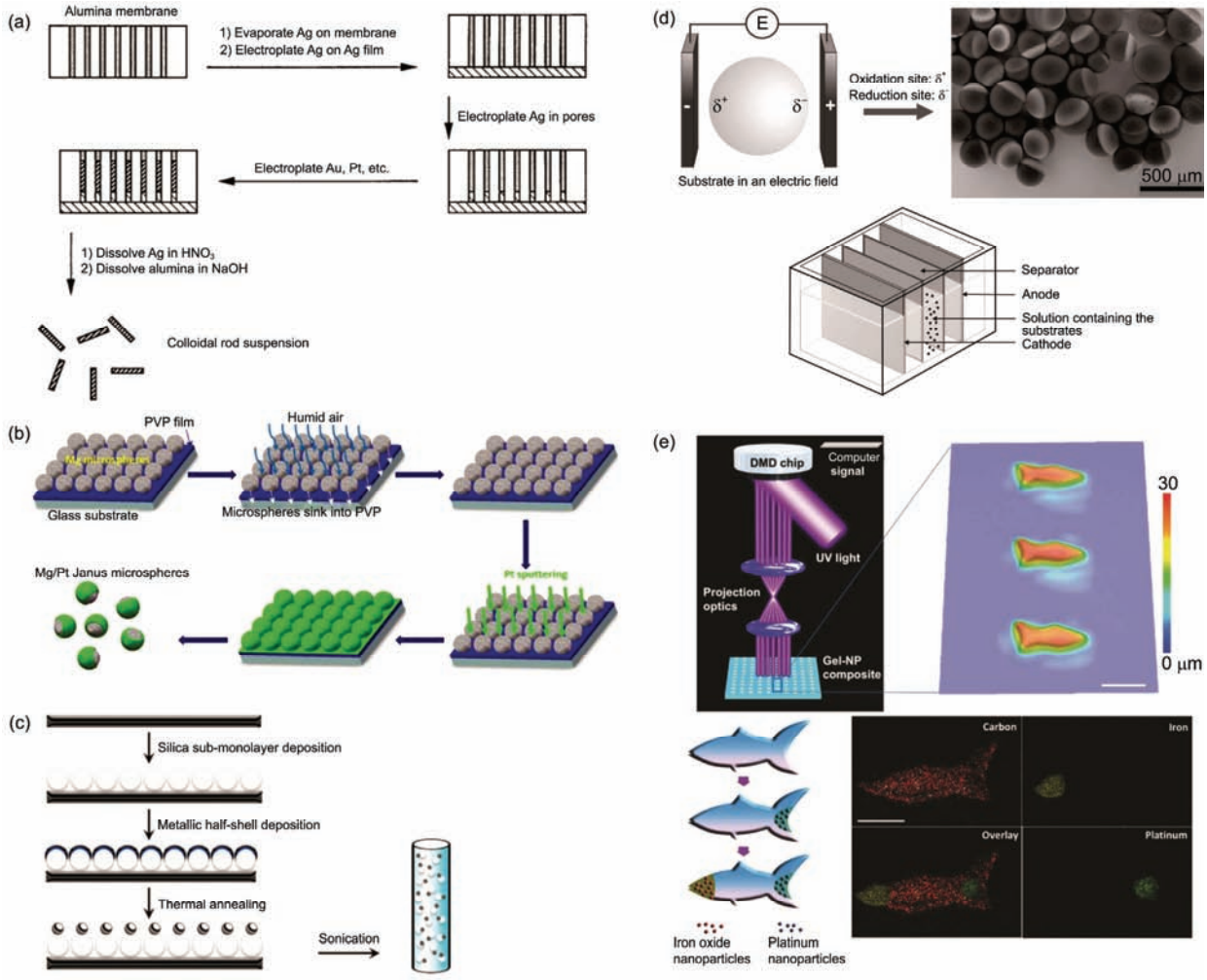

图 2 (网络版彩色)(a) 电化学法制备双金属棒[45]; (b) 表面非对称改性制备Mg/Pt双面神微球[46]; (c) 制备自驱动的球形SiO_2-Pt二聚体[47]; (d) 两极电沉积制备双面神粒子[48]; (e) 3D打印技术制备鱼形马达[49]

Figure 2 (Color online) (a) Electrochemical synthesis of the metal rods[45]. (b) Schematic diagram of the fabrication of Mg/Pt Janus microspheres by a simple asymmetric modification process[46]. (c) Synthesis of the self-propelled spherical SiO_2-Pt dimers[47]. (d) Bipolar electrodeposition for the synthesis of Janus particles[48]. (e) Schematic illustration of 3D printing technology to fabricate microfish[49]

应会在导电粒子的一侧发生. 采用这样的方式, 可以在碳管、碳珠和银纳米线上非对称地沉积金和氯化银(图2(d)). 随着3D打印的迅速发展, Wang课题组[49]采用3D打印技术制备了不同形状的鱼形微米马达, 并使用含有不同纳米粒子的“墨水”, 打印出鱼头含有磁性纳米粒子、鱼身含有聚丁二炔纳米粒子、鱼尾含有Pt纳米粒子的微米马达(图2(e)).

双面神结构的制备解决了微纳米马达运动的问题, 为了使双面神结构的微纳米马达具备运动的可控和功能化. 在结构设计中会引入一些磁性层或是功能层, 通过外场的调控引导运动方向或释放行为. Wang课题组[62]在镀层中引入了镍, 可以通过磁场精确地控制马达的运动方向(图3(a)). 他们在得到了含有磁性成分的Au/Ni/Au/Pt纳米线和SiO_2/Ni/Pt粒子后, 在磁场的牵引下能够在双氧水中定向运动, 并利用马达作为运动的掩膜板[63], 可以在光刻胶上制备高精度图案(图3(b)). 后来, Sánchez课题组[64]发现自扩散泳运动的SiO_2/Pt微米马达可以以边界图案作为导向引导发动机的运动. 在实验中, 他们分别设计了直线阶梯边界(I)、带有直角的H形边界(II)和圆柱形边界(III), 马达均能很好地沿着边界运动, 为引导微纳米马达的运动提供了一个新思路(图3(c)). 本课题组[65]在Mg/Pt双面神微米马达的基础上, 在Pt一侧加入了具有温敏响应的水凝胶——聚(*N*-异丙基丙烯酰

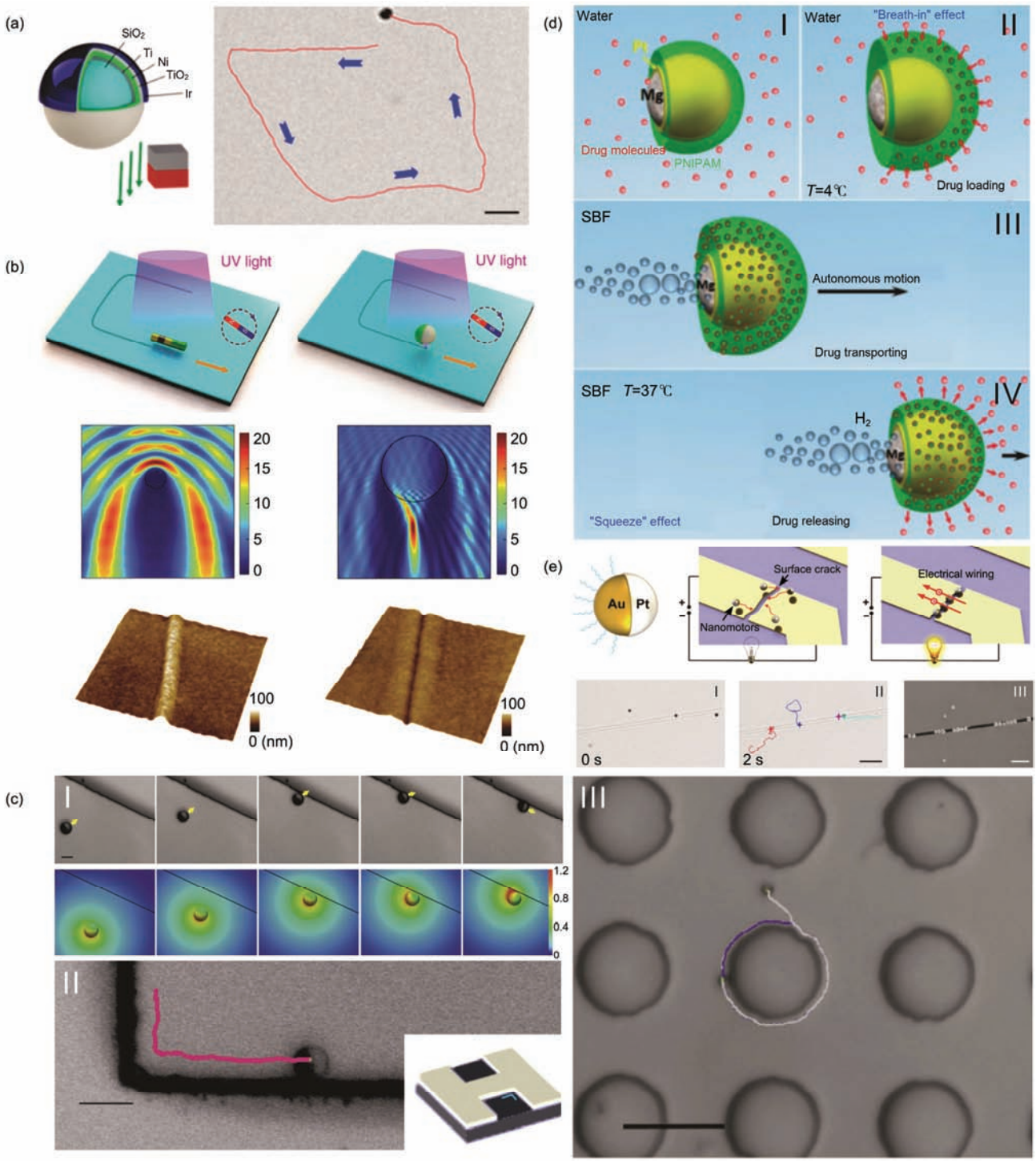

图 3 (网络版彩色)(a) Ir-TiO_2-Ni-Ti-SiO_2多层双面神马达在磁场下的运动控制[62]; (b) 使用纳米线马达和双面神球形马达作为自驱动的纳米掩膜板进行光刻的示意图[63]; (c) 双面神马达在不同图案下的导向运动[64]; (d) Mg/Pt-PNIPAM双面神马达的药物装载(I, II)、运输(III)和释放(IV)[65]; (e) 通过人工纳米马达寻找和修复由机械裂纹引起的断路[66]

Figure 3 (Color online) (a) Schematic of the magnetic control of multilayer Ir-TiO_2-Ni-Ti-SiO_2 Janus micromotors[62]. (b) Schematic of nanomotor lithography by using a nanowire motor and Janus sphere motor as a self-propelled nanomask[63]. (c) Guidance of Janus microswimmers with different patterns[64]. (d) Demonstration of the drug loading (I, II), transporting (III), and releasing (IV) behaviors of the Mg/Pt-PNIPAM Janus micromotors[65]. (e) Seeking and repairing microscopic mechanical cracks by artificial nanomotors to effectively restore conductivity[66]

胺)(PNIPAM). 利用PNIPAM的温敏特性, 将马达置于低温环境中, PNIPAM会吸水膨胀从而将“药物分子”(FITC)装载到马达上; 随后将温度升高时, PNIPAM会排水收缩, FITC就会释放出去; 因此, 利用该性质制备了可温控释药的微米马达(图3(d)). Wang课题组[66]直接使用Au/Pt双面神马达的运动寻找电路中的断路处, 并且填补在断开的狭缝中, 利用马达自身良好的导电性修复电路(图3(e)).

3 多层管状结构马达

多层管状结构是指由组成不同的两层或两层以上的膜卷曲形成的管状结构. 这种结构通常先在模板上分别沉积不同组成的薄膜, 然后再将模板进行刻蚀得到. 利用这种多层管状结构来构建微纳米马达, 只需要控制反应活性层与惰性层的沉积顺序, 确保管内侧具有反应活性, 外表面是惰性层. 利用管内外非对称的化学反应即能形成非对称场, 从而得到多层结构微纳米马达[15,67]. Wang课题组[68]采用模板辅助的方法制备了Au-Pt锥形管状微米马达(图4(a)). 首先将银纳米线刻蚀成锥状, 然后依次沉积Pt和Au, 最后再将Ag刻蚀掉就得到了锥形管状马达. 层层自组装技术也是制备多层管状微纳米马达常用的方法, 贺强课题组[69]使用多孔膜作为模板, 将一些带电的聚合物溶解后依次吸附在膜孔内表面, 最后再将改性后的Pt纳米粒子吸附在最里层, 溶剂完全挥发后刻蚀掉模板就得到了内壁镶嵌有Pt纳米粒子的多层管状马达(图4(b)). 梅永丰课题组[70]发展了一种薄膜自卷曲法制备管状微米马达(图4(c)), 在聚合物膜表面依次均匀地镀上各种无机纳米薄膜, 然后选用合适的溶剂使聚合物膜溶解, 多层的无机纳米薄膜就会在内应力的作用下自卷曲形成多层管. 通过设计镀层顺序, 惰性层在管的最外层, 活性层在管的内层. 他们用该方法制备了很多复合管状马达[16]. 在多层管的制备方法中, 电化学沉积仍然是一种较为普遍的方法. Wang课题组[71~73]采用电化学沉积的方法制备了很多聚电解质与金属复合的多层管状微米马达(图4(d)), 能够在双氧水或酸中很好地运动.

多层管状微纳米马达由于其管内独特的受限空间和管外壁较大的表面积, 具有一些非常特殊的运动控制手段和应用. Wang课题组[74]制备了PEDOT/

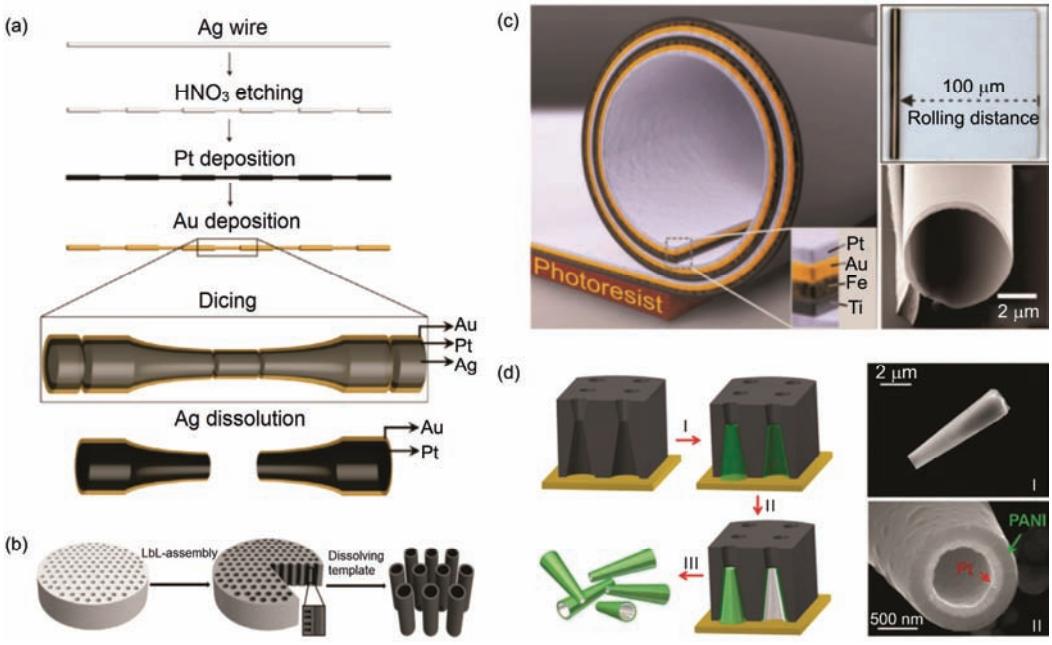

图 4 (网络版彩色)(a) 模板辅助法制备锥形管状微米马达[68]; (b) 层层自组装法制备聚电解质多层管状纳米火箭[69]; (c) 在光刻胶上采用自卷曲法制备Pt/Au/Fe/Ti多层管状马达[70]; (d) 电化学法制备双层PANI/Pt微米管[71]

Figure 4 (Color online) (a) Schematic illustrating the steps involved in the template-assisted preparation of the tubular microcone engine[68]. (b) Fabrication of polyelectrolyte multilayer with nanorockets through the nanoporous template-assisted layer-by-layer (LbL) assembly[69]. (c) Schematic diagram of a rolled-up microtube consisting of Pt/Au/Fe/Ti multilayers on a photoresist sacrificial layer[70]. (d) Preparation of bilayer PANI/Pt microtubes through electrochemical growth[71]

Ni/Pt微米管状马达(图5(a)), 该马达不仅能够在磁场下定向运动, 而且能够通过超声影响管内气泡的生长, 控制马达的运动速度. Sánchez课题组[75]将PNIPAM薄膜加入到多层管组分中, 利用PNIPAM随着温度变化展现出来的伸缩特性, 使薄膜在低温时卷成管状开始运动, 在高温时又展开形成膜停止运动(图5(b)). 通过对多层管状马达的外层进行修饰, 能够实现癌细胞、核酸、细菌的分离(图5(c)), 蛋白质的运输(图5(d)), 分子识别和环境检测与修复(图5(e))等功能[76~86].

双面神结构和多层管状结构的微纳米马达能够赋予马达良好的运动性能和功能化, 但是制备过程相当复杂, 往往需要进行多层的修饰和改性.

4 各向异性单组分结构马达

各向异性单组分结构是指组成单一但结构不对称的微纳米粒子、管或罐等结构. 由于气体分子在非对称结构表面成核的难易程度不同, 因此可以在其周围形成非对称场, 驱使其自主运动. 这类各向异性单组分结构微纳米马达的出现使马达的结构和制备方法得到了简化. Pumera课题组[87]直接使用购买的Ag和MnO_2微米粒子在双氧水中展示了较好的运动行为, 这些粒子由于结构的各向异性导致了气泡在粒子上有很多不同的成核位点, 气体分子会选择在易于成核的地方成核生长. 然而, 该非规则的结构各向异性的马达并不能很好地帮助我们对运动进行控制以及不具备良好的重复性, 在实际应用中会受到限制.

本课题组[14]采用同轴纺丝法制备了具有结构规则的单组分TiO_2微米管(图6(a)), 在紫外光照射下, 能够分解双氧水产生氧气推动马达的运动. 通过观察发现, 气泡只会从管内释放出来. 通过模拟计算得出结论, TiO_2微米管在紫外光照射时, 管内壁和外壁都会分解双氧水产生氧气分子, 但是管外壁的凸面

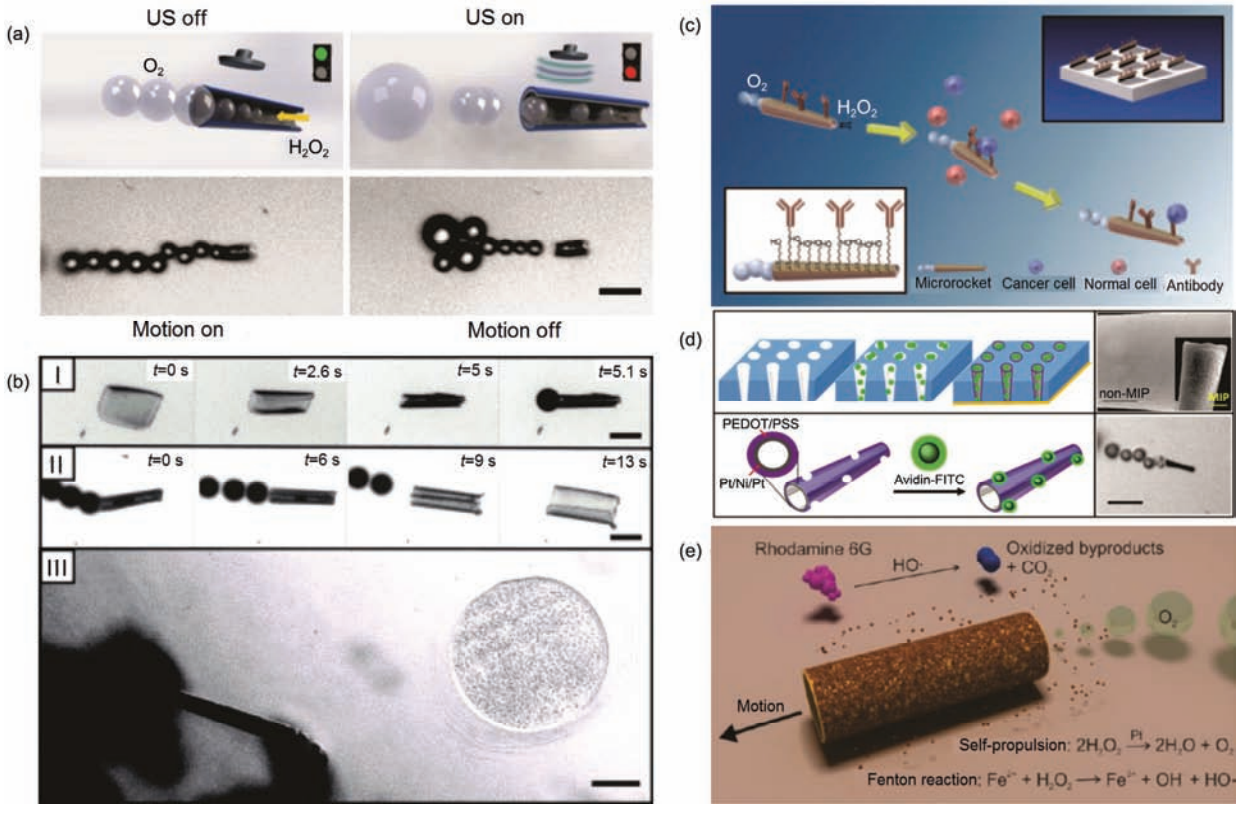

图 5 (网络版彩色)(a) 超声控制PEDOT/Ni/Pt马达的运动[74]; (b) 温度控制聚合物基Pt催化马达的运动[75]; (c) 微米火箭捕捉和分离癌细胞[76]; (d) 分子印迹微米马达捕捉和运输蛋白质[77]; (e) 多功能马达降解污染物[78]

Figure 5 (Color online) (a) Ultrasound modulated motion of a chemically powered PEDOT/Ni/Pt microengine[74]. (b) Temperature controlled motion of a polymeric Pt-jet[75]. (c) Microrockets for capture and isolation of cancer cells[76]. (d) MIP-based micromotor and the strategy for capture and transport the target protein[77]. (e) Schematic process for the degradation of pollutants water by multifunctional micromotors[78]

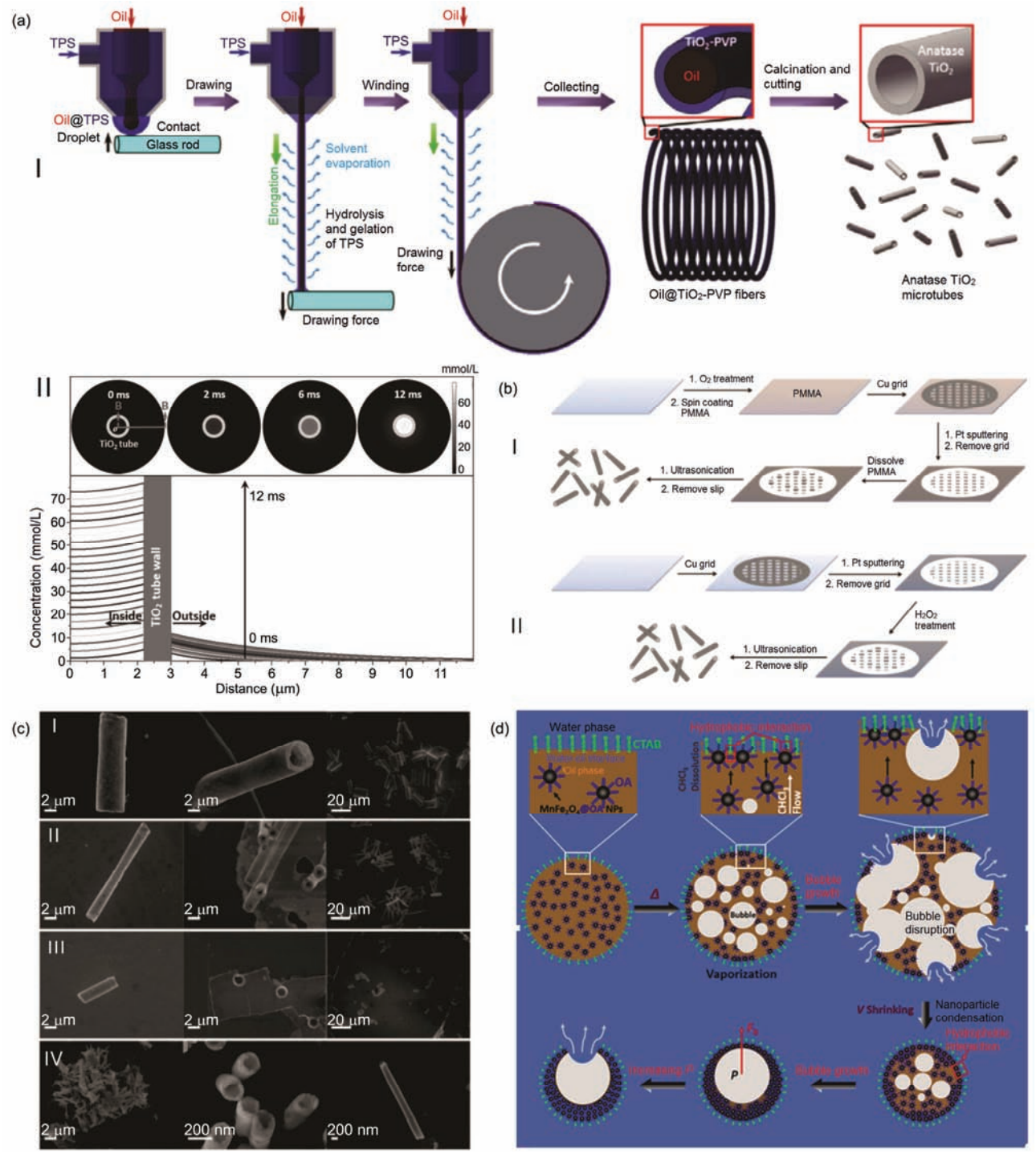

图 6 (网络版彩色)(a) 纺丝法制备TiO_2管的示意图(I)和不同扩散时间时管内外的氧气浓度的径向和轴向分布图(II)[14]; (b) 卷曲法制备Pt管微米马达, 采用聚甲基丙烯酸甲酯(PMMA)作为牺牲层溶解后卷曲(I)和H_2O_2中超声卷曲(II)[88]; (c) 采用各种孔径的多孔膜制备得到的 4 种Pt管状马达的扫描电子显微镜图(SEM)[89]; (d) $MnFe_2O_4$罐状微米马达的成型机理[90]

Figure 6 (Color online) (a) Schematics to demonstrate the preparation of the TiO_2 microtubes by a dry spinning method (I), the radial and axial concentration distribution of O_2 in the confined void and outside space of the TiO_2 tube at different diffusion time(II)[14]. (b) Depiction of steps used during fabrication of Pt roll-up microengines via TEM grid template/PMMA sacrificial layer route (I) or TEM grid template/H_2O_2 assisted lift-off route (II) [88]. (c) SEM images of the four types of prepared Pt micro/nanotubes using membrane templates with different pore sizes[89]. (d) Schematic illustration for the formation mechanism of the pot-like $MnFe_2O_4$ micromotors[90]

不利于气泡的成核，释放出来的氧气分子很快向外扩散. 而管内的受限空间利于气泡的成核生长，因此只能观察到气泡从管内释放出去. 这就为实现结构规则的各向异性单组分微纳米马达的运动提供了理论依据，只要能制备出合适孔径的单组分管或是提供一个利于气泡成核的凹面结构就可以满足马达的运动.

薄膜自卷曲法同样可以制备出单组分的管状马达，Zhao等人[88]和Giudicatti等人[91]采用卷曲法分别制备了单组分的TiO_2管和Pt管(图6(b)). 电化学沉积法同样也能制备单组分的管状马达，Pumera课题组[89]采用模板辅助电沉积法(图6(c))，用多孔的聚碳酸酯作为模板，能够制备出各种孔径和尺寸的Pt管. 不仅单组分的微米管能够运动，而且利于气泡成核的凹面结构的单层罐状粒子也能够很好的运动. 本课题组[90]提出了“气泡模板”辅助纳米粒子组装法(图6(d))快速制备单层中空$MnFe_2O_4$基的罐状微米马达. $MnFe_2O_4$@OA纳米粒子能够催化分解双氧水，由于罐状结构内部利于气泡成核，因此可以看到氧气泡不断地从罐口处喷出.

这些各向异性单组分结构的微米马达能够一步成型，根据气泡在不同面上成核的难易程度形成了非对称场，而且不需要进一步修饰改性就能够实现马达的功能化. 单组分的TiO_2管[14]可以通过紫外光控制运动的起停，而且反应迅速(图7(a)). $MnFe_2O_4$基罐状微米马达[90]除了能够通过磁场导向外，还可以通过纳米粒子表面的油酸分子起到很好地吸附油滴的效果(图7(b)).

5 各向同性微纳米粒子马达

非对称的微纳米结构能够通过在其周围产生的化学反应或物理效应来构建非对称场，从而实现自主运动. 但是正如前面描述的那样，这类结构的制备通常较为复杂，难以宏量制备. 如果各向同性粒子也能在粒子两边发生非对称的化学反应，建立非对称场，这样将极大地简化马达的结构和制备方法. 沿着该思路，本课题组[92]最近利用紫外光在TiO_2微米粒子中的有限穿透深度，在各向同性TiO_2粒子两侧构建出非对称光致化学反应，发展出了各向同性半导体光控微纳米马达. 这种TiO_2微米马达受到光照会在粒子两侧形成光催化产物的浓度差，当产物的浓度差积累到一定程度时，足以推动TiO_2微米粒子沿着光照方向前进. 调节光照方向，粒子的运动轨迹会随着发生变化. 接着，他们发现其他的一些光催化材料如ZnO，Ag_3PO_4和CdS也有类似的性质. 通过改变外场的施加条件就能实现各向同性粒子的正趋光与负趋光直线运动(图8).

为了展示TiO_2粒子的负趋光特性，采用多个方向的光照，使粒子能够按照预先设计的路线前进，准确到达目的地(图9(a)). 另外，在光控泳动吸引(phoretic attraction)的作用下，各向同性TiO_2马达还具有可控装载、运输和卸载微纳米货物的能力. 如图9(b)所示，

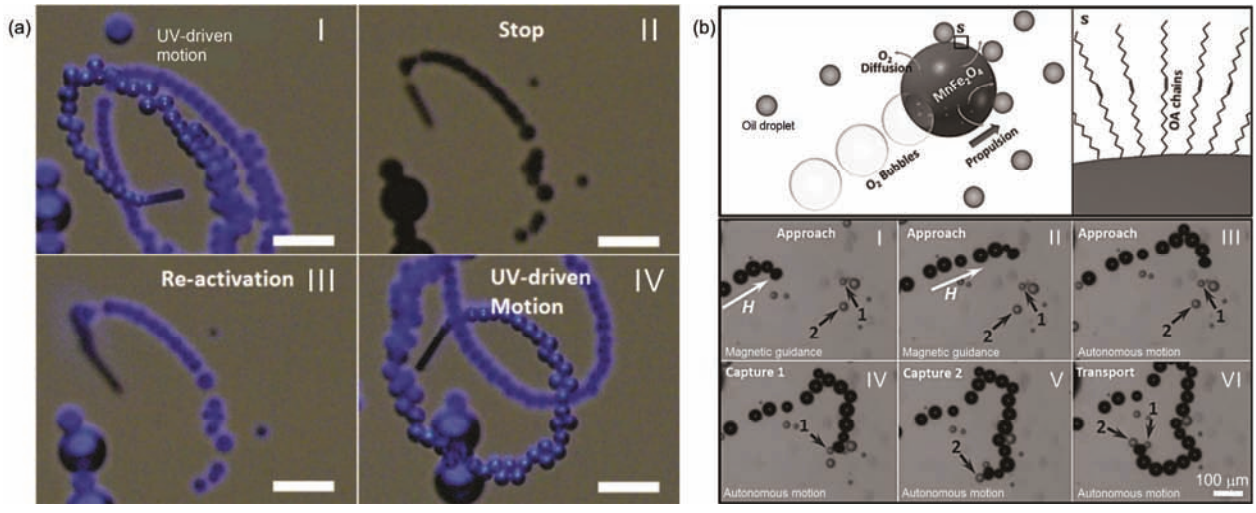

图 7 (网络版彩色)(a) 单组分TiO_2微米马达的光控运动时序图[14]; (b) $MnFe_2O_4$罐状微米马达通过其疏水表面移除油滴[90]

Figure 7 (Color online) (a) Time-lapse images of the light-controlled motion of a typical single-component TiO_2 microengine[14]. (b) The removal of oil droplets by the pot-like $MnFe_2O_4$ micromotor due to their hydrophobic outer surfaces[90]

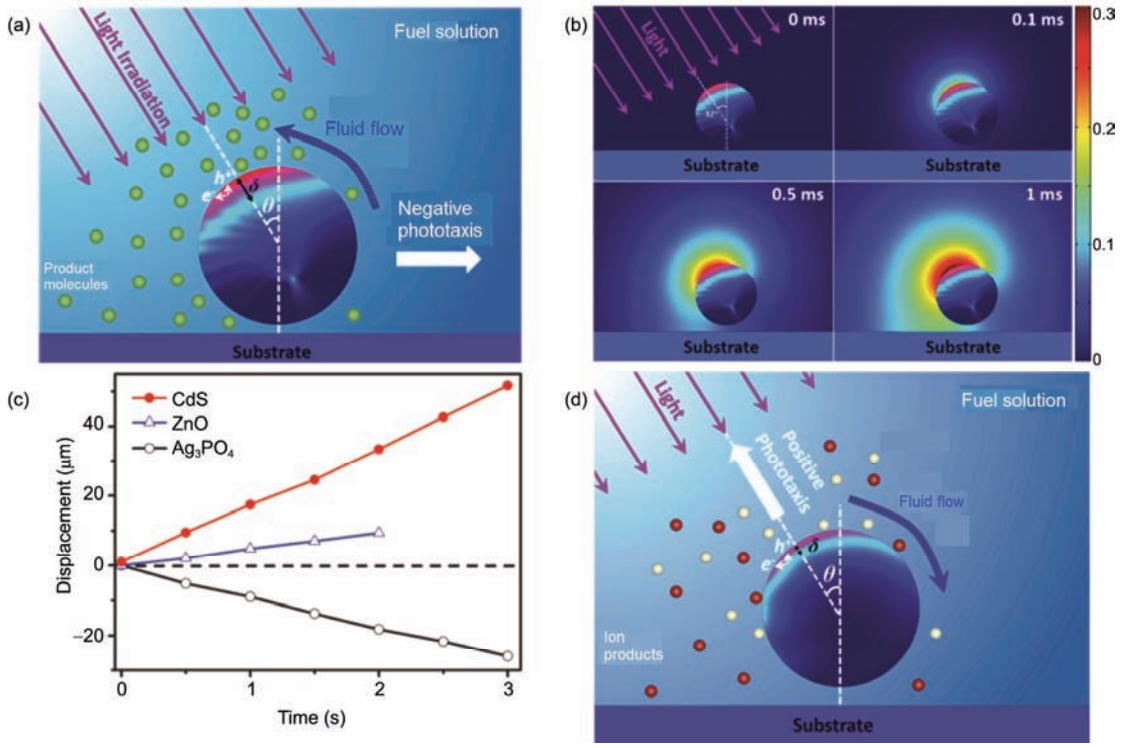

图 8 (网络版彩色)(a) 各向同性的TiO_2微米马达在紫外光照下的负趋光运动机理图; (b) 在不同的照射时间时对 1.2 μm TiO_2粒子周围氧气浓度分布的数值模拟; (c) Ag_3PO_4, ZnO和CdS微米马达分别在紫外光(365 nm, 1 W/cm^2)或蓝光(420 nm, 0.1 W/cm^2)照射下在*X*-*Y* 平面内的位移; (d) ZnO微米马达正趋光运动的机理图[92]

Figure 8 (Color online) (a) Schematic diagram of the linear negative phototaxis of an isotropic TiO_2 micromotor under the UV irradiation. (b) Numerical simulation results of the distribution of O_2 concentration (mmol/L) around a 1.2-μm-diameter TiO_2 microsphere at different irradiation time intervals. (c) Displacement in the *X*-*Y* plane of Ag_3PO_4, ZnO and CdS micromotors under the irradiation of UV (365 nm, 1 W/cm^2) or blue light (420 nm, 0.1 W/cm^2). (d) Schematic diagram of the positive phototaxis of a ZnO micromotor[92]

由于这种各向同性马达的定向运动特性, 能够在紫外光照下按照设定的路线准确地将二氧化硅粒子搬运到预定目的地. 通过光照条件的改变, 实现了各向同性粒子的定向运动, 并且还能够执行复杂的任务, 采用一个外场完成了以前需要多个外场才能完成的任务, 这是自驱动微纳米马达发展史上一个重大发现.

6 结论与展望

自驱动微纳米马达的驱动机理可以分为气泡反冲驱动和自泳驱动, 它们的共同点在于构建一个非对称场. 根据这样的思想, 自驱动微纳米马达的发展经历了从双面神结构和多层管状结构, 到各向异性单组分结构和各向同性粒子的演变. 双面神结构用简单明了的方式成功地构筑了非对称场, 实现了微纳米马达的运动. 但是它的制备方法通常十分繁琐, 而且在运动过程中极易受到布朗运动的影响而发生翻转或偏移, 运动方向无法保持, 需要通过外加磁性层等手段才能控制运动轨迹. 多层管状结构马达具有与双面神马达类似的设计原理, 它通过控制沉积顺序使活性层处在管内侧, 惰性层包覆在管外, 利用管内外的反应活性差异来构建非对称场实现自主运动. 然而, 多层管状马达的制备也较复杂. 与此相比, 各向异性单组分结构能实现微纳米马达的一步成型, 具有大规模制备的条件. 但由于结构的各向异性, 它依旧受布朗运动的影响而不易控制运动方向. 光控各向同性半导体粒子马达的出现打破了构建非对称场传统思想的禁锢. 这不但极大地简化了微纳米马达的制备方法, 而且通过改变外场的施加方式实现了对马达运动速率和方向的同时控制. 这激励人们进一步探索对电、磁和超声等外场响应的各向同性粒子马达及其定向运动控制策略. 从自驱动微纳米马达的发展历程可以看出, 微纳米马达的结构设计在逐渐简化, 功能也在不断完善. 比如, 运动速度和状态能够通过燃料浓度、外场条件等很好地调控;

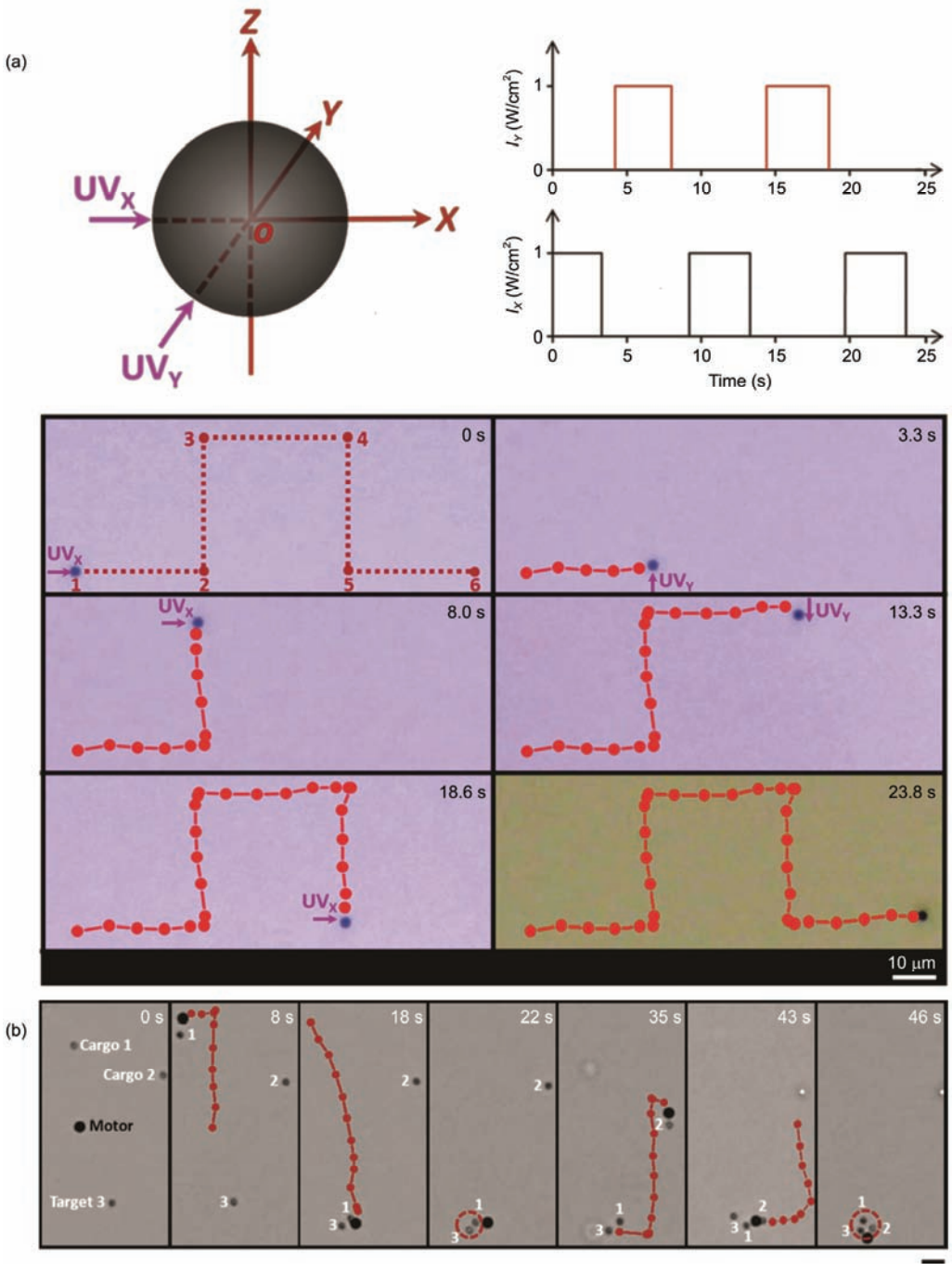

图 9 (网络版彩色)(a) TiO_2 微米马达在紫外光控制下按照设定路线运动的时序图和轨迹; (b) TiO_2 微米马达按照设计路线搬运货物[92]

Figure 9 (Color online) (a) Time-lapse images and the motion trajectory of a TiO_2 micromotor controlled by UV light in designed route. (b) A TiO_2 micromotor transports cargoes in designed route[92]

运动方向可以通过外加磁场、光、电场等手段进行远程精确控制; 通过与其他材料的结合, 实现了蛋白质、癌细胞等的快速分离、药物运输、环境的检测与修复等等一系列非常有意义的功能. 然而, 目前所取得的成果还远满足不了实现微纳米马达实际应用的要求. 这主要由3个方面的因素导致: (1) 能量转换效率非常低, 大部分自驱动微纳米马达的能量转化效率仅在10^{-9}~10^{-10}数量级, 绝大部分的能量都没有转化成动能, 使马达的运动速度相对较低, 难以在一些黏度较高的介质如血液中运动. 这是由微纳米马达

的运动机理和微纳米粒子在低雷诺数环境中运动的性质等决定的. 因此, 自驱动微纳米马达未来的方向之一是建立并完善微纳米粒子在流体中的运动模型, 优化设计马达的结构, 提高马达的能量转换效率. (2) 大多数自驱动微纳米马达的运动严重依赖一些与生物相容性较差的燃料, 难以满足马达在生物环境中的应用. 目前, 能够在模拟体液、血浆和血液等环境中运动的自驱动马达都属于反应消耗型, 运动寿命短的问题极大地限制了它们的应用. 因此, 发展新的驱动机理或马达, 提高生物相容的马达的运动寿命仍然是微纳米马达未来发展的重点. (3) 目前的微纳米马达需要借助外场等来引导运动方向, 在实际应用时会带来一些困难. 当需要操作的范围远大于外场所能施加的范围时, 马达就会失去引导, 变成“无头苍蝇”. 因此, 未来的微纳米马达需要实现“自探寻”功能. 通过马达自身“感知”外界环境, 得到反馈后做出反应, 根据环境引导马达的运动和执行任务, 达到智能化的标准. 总之, 通过不断的探索与发现, 未来的微纳米马达有望应用在生物医药、环境治理和微工程等领域.

参考文献

1 Wang J. Can man-made nanomachines compete with nature biomotors? ACS Nano, 2009, 3: 4–9
2 Wang J, Gao W. Nano/microscale motors: Biomedical opportunities and challenges. ACS Nano, 2012, 6: 5745–5751
3 Solovev A A, Xi W, Gracias D H, et al. Self-propelled nanotools. ACS Nano, 2012, 6: 1751–1756
4 Orozco J, García-Gradilla V, D'Agostino M, et al. Artificial enzyme-powered microfish for water-quality testing. ACS Nano, 2013, 7: 818–824
5 Guix M, Orozco J, García M, et al. Superhydrophobic alkanethiol-coated microsubmarines for effective removal of oil. ACS Nano, 2012, 6: 4445–4451
6 Wang J, Manesh K M. Motion control at the nanoscale. Small, 2010, 6: 338–345
7 Gao W, Wang J. The environmental impact of micro/nanomachines: A review. ACS Nano, 2014, 8: 3170–3180
8 Singh V V, Wang J. Nano/micromotors for security/defense applications: A review. Nanoscale, 2015, 7: 19377–19389
9 Guix M, Mayorga-Martinez C C, Merkoci A. Nano/micromotors in (bio)chemical science applications. Chem Rev, 2014, 114: 6285–6322
10 Gibbs J G, Zhao Y P. Autonomously motile catalytic nanomotors by bubble propulsion. Appl Phys Lett, 2009, 94: 163104
11 Yang M, Wysocki A, Ripoll M. Hydrodynamic simulations of self-phoretic microswimmers. Soft Matter, 2014, 10: 6208–6218
12 Wang H, Pumera M. Fabrication of micro/nanoscale motors. Chem Rev, 2015, 115: 8704–8735
13 Sanchez S, Soler L, Katuri J. Chemically powered micro- and nanomotors. Angew Chem Int Ed, 2015, 54: 1414–1444
14 Mou F, Li Y, Chen C, et al. Single-component TiO_2 tubular microengines with motion controlled by light-induced bubbles. Small, 2015, 11: 2564–2570
15 Li J, Rozen I, Wang J. Rocket science at the nanoscale. ACS Nano, 2016, 10: 5619–5634
16 Mei Y, Solovev A A, Sanchez S, et al. Rolled-up nanotech on polymers: From basic perception to self-propelled catalytic microengines. Chem Soc Rev, 2011, 40: 2109–2119
17 Wang W, Duan W, Ahmed S, et al. From one to many: Dynamic assembly and collective behavior of self-propelled colloidal motors. Acc Chem Res, 2015, 48: 1938–1946
18 Wang W, Duan W, Ahmed S, et al. Small power: Autonomous nano- and micromotors propelled by self-generated gradients. Nano Today, 2013, 8: 531–554
19 Lin X, Wu Z, Wu Y, et al. Self-propelled micro-/nanomotors based on controlled assembled architectures. Adv Mater, 2016, 28: 1060–1072
20 Ismagilov R F, Schwartz A, Bowden N, et al. Autonomous movement and self-assembly. Angew Chem Int Ed, 2002, 114: 674–676
21 Manjare M, Yang B, Zhao Y P. Bubble-propelled microjets: Model and experiment. J Phys Chem C, 2013, 117: 4657–4665
22 Li J, Huang G, Ye M, et al. Dynamics of catalytic tubular microjet engines: Dependence on geometry and chemical environment. Nanoscale, 2011, 3: 5083–5089
23 Paxton W F, Kistler K C, Olmeda C C, et al. Catalytic nanomotors: Autonomous movement of striped nanorods. J Am Chem Soc, 2004, 126: 13424–13431
24 Mou F, Kong L, Chen C, et al. Light-controlled propulsion, aggregation and separation of water-fuelled TiO_2/Pt Janus submicromotors and their “on-the-fly” photocatalytic activities. Nanoscale, 2016, 8: 4976–4983
25 Hong Y, Diaz M, Córdova-Figueroa U M, et al. Light-driven titanium-dioxide-based reversible microfireworks and micromotor/micropump systems. Adv Funct Mater, 2010, 20: 1568–1576

26 Pavlick R A, Sengupta S, McFadden T, et al. A polymerization-powered motor. Angew Chem Int Ed, 2011, 50: 9374–9377
27 Toyota T, Maru N, Hanczyc M M, et al. Self-propelled oil droplets consuming “fuel” surfactant. J Am Chem Soc, 2009, 131: 5012–5013
28 Xuan M, Wu Z, Shao J, et al. Near infrared light-powered Janus mesoporous silica nanoparticle motors. J Am Chem Soc, 2016, 138: 6492–6497
29 Gao W, Sattayasamitsathit S, Wang J. Catalytically propelled micro-/nanomotors: How fast can they move? Chem Rec, 2012, 12: 224–231
30 Pumera M. Electrochemically powered self-propelled electrophoretic nanosubmarines. Nanoscale, 2010, 2: 1643–1649
31 Paxton W F, Sen A, Mallouk T E. Motility of catalytic nanoparticles through self-generated forces. Chem A Eur J, 2005, 11: 6462–6470
32 Wang Y, Hernandez R M, Bartlett D J, et al. Bipolar electrochemical mechanism for the propulsion of catalytic nanomotors in hydrogen peroxide solutions. Langmuir, 2006, 22: 10451–10456
33 Dong R, Zhang Q, Gao W, et al. Highly efficient light-driven TiO_2-Au Janus micromotors. ACS Nano, 2015, 10: 839–844
34 Ibele M, Mallouk T E, Sen A. Schooling behavior of light-powered autonomous micromotors in water. Angew Chem Int Ed, 2009, 48: 3308–3312
35 Zhao G, Pumera M. Macroscopic self-propelled objects. Chem Asia J, 2012, 7: 1994–2002
36 Chaudhury M K, Whitesides G M. How to make water run uphill. Science, 1992, 256: 1539–1541
37 Lee S W, Laibinis P E. Directed movement of liquids on patterned surfaces using noncovalent molecular adsorption. J Am Chem Soc, 2000, 122: 5395–5396
38 Sumino Y, Magome N, Hamada T, et al. Self-running droplet: Emergence of regular motion from nonequilibrium noise. Phys Rev Lett, 2005, 94: 068301
39 Kohira M I, Hayashima Y, Nagayama M, et al. Synchronized self-motion of two camphor boats. Langmuir, 2001, 17: 7124–7129
40 Bassik N, Abebe B T, Gracias D H. Solvent driven motion of lithographically fabricated gels. Langmuir, 2008, 24: 12158–12163
41 Sharma R, Chang S T, Velev O D. Gel-based self-propelling particles get programmed to dance. Langmuir, 2012, 28: 10128–10135
42 Zhang H, Duan W, Liu L, et al. Depolymerization-powered autonomous motors using biocompatible fuel. J Am Chem Soc, 2013, 135: 15734–15737
43 Wang L, Yuan B, Lu J, et al. Self-propelled and long-time transport motion of PVC particles on a water surface. Adv Mater, 2016, 28: 4065–4070
44 Wu Z, Si T, Gao W, et al. Superfast near-infrared light-driven polymer multilayer rockets. Small, 2016, 12: 577–582
45 Martin B R, Dermody D J, Reiss B D, et al. Orthogonal self-assembly on colloidal gold-platinum nanorods. Adv Mater, 1999, 11: 1021–1025
46 Mou F, Chen C, Ma H, et al. Self-propelled micromotors driven by the magnesium-water reaction and their hemolytic properties. Angew Chem Int Ed, 2013, 52: 7208–7212
47 Valadares L F, Tao Y G, Zacharia N S, et al. Catalytic nanomotors: Self-propelled sphere dimers. Small, 2010, 6: 565–572
48 Loget G, Roche J, Kuhn A. True bulk synthesis of Janus objects by bipolar electrochemistry. Adv Mater, 2012, 24: 5111–5116
49 Zhu W, Li J, Leong Y J, et al. 3D-printed artificial microfish. Adv Mater, 2015, 27: 4411–4417
50 Zhao G, Ambrosi A, Pumera M. Self-propelled nanojets via template electrodeposition. Nanoscale, 2013, 5: 1319–1324
51 Liu R, Sen A. Autonomous nanomotor based on copper-platinum segmented nanobattery. J Am Chem Soc, 2011, 133: 20064–20067
52 Fournier-Bidoz S, Arsenault A C, Manners I, et al. Synthetic self-propelled nanorotors. Chem Commun, 2005, 441–443
53 Teo W Z, Wang H, Pumera M. Beyond platinum: Silver-catalyst based bubble-propelled tubular micromotors. Chem Commun, 2016, 52: 4333–4336
54 Golestanian R, Liverpool T B, Ajdari A. Propulsion of a molecular machine by asymmetric distribution of reaction products. Phys Rev Lett, 2005, 94: 220801
55 Howse J R, Jones R A, Ryan A J, et al. Self-motile colloidal particles: From directed propulsion to random walk. Phys Rev Lett, 2007, 99: 048102
56 Gao W, Pei A, Wang J. Water-driven micromotors. ACS Nano, 2012, 6: 8432–8438
57 Gao W, D’Agostino M, Garcia-Gradilla V, et al. Multi-fuel driven Janus micromotors. Small, 2013, 9: 467–471
58 Gao W, Feng X, Pei A, et al. Seawater-driven magnesium based Janus micromotors for environmental remediation. Nanoscale, 2013, 5: 4696–4700
59 Baraban L, Makarov D, Streubel R, et al. Catalytic Janus motors on microfluidic chip: Deterministic motion for targeted cargo delivery. ACS Nano, 2012, 6: 3383–3389
60 Ma X, Hahn K, Sanchez S. Catalytic mesoporous Janus nanomotors for active cargo delivery. J Am Chem Soc, 2015, 137: 4976–4979
61 Lee T C, Alarcon-Correa M, Miksch C, et al. Self-propelling nanomotors in the presence of strong brownian forces. Nano Lett, 2014, 14: 2407–2412

62 Gao W, Pei A, Dong R, et al. Catalytic iridium-based Janus micromotors powered by ultralow levels of chemical fuels. J Am Chem Soc, 2014, 136: 2276–2279
63 Li J, Gao W, Dong R, et al. Nanomotor lithography. Nat Commun, 2014, 5: 5026
64 Simmchen J, Katuri J, Uspal W E, et al. Topographical pathways guide chemical microswimmers. Nat Commun, 2016, 7: 10598
65 Mou F, Chen C, Zhong Q, et al. Autonomous motion and temperature-controlled drug delivery of Mg/Pt-poly(*N*-isopropylacrylamide) Janus micromotors driven by simulated body fluid and blood plasma. ACS Appl Mater Interfaces, 2014, 6: 9897–9903
66 Li J, Shklyaev O E, Li T, et al. Self-propelled nanomotors autonomously seek and repair cracks. Nano Lett, 2015, 15: 7077–7085
67 Huang G, Wang J, Mei Y. Material considerations and locomotive capability in catalytic tubular microengines. J Mater Chem, 2012, 22: 6519
68 Manesh K M, Cardona M, Yuan R, et al. Template-assisted fabrication of salt-independent catalytic tubular microengines. ACS Nano, 2010, 4: 1799–1804
69 Wu Z, Wu Y, He W, et al. Self-propelled polymer-based multilayer nanorockets for transportation and drug release. Angew Chem Int Ed, 2013, 52: 7000–7003
70 Solovev A A, Mei Y, Bermudez Urena E, et al. Catalytic microtubular jet engines self-propelled by accumulated gas bubbles. Small, 2009, 5: 1688–1692
71 Gao W, Sattayasamitsathit S, Orozco J, et al. Highly efficient catalytic microengines: Template electrosynthesis of polyaniline/platinum microtubes. J Am Chem Soc, 2011, 133: 11862–11864
72 Gao W, Sattayasamitsathit S, Uygun A, et al. Polymer-based tubular microbots: Role of composition and preparation. Nanoscale, 2012, 4: 2447–2453
73 Gao W, Uygun A, Wang J. Hydrogen-bubble-propelled zinc-based microrockets in strongly acidic media. J Am Chem Soc, 2012, 134: 897–900
74 Xu T, Soto F, Gao W, et al. Ultrasound-modulated bubble propulsion of chemically powered microengines. J Am Chem Soc, 2014, 136: 8552–8555
75 Magdanz V, Stoychev G, Ionov L, et al. Stimuli-responsive microjets with reconfigurable shape. Angew Chem Int Ed, 2014, 53: 2673–2677
76 Balasubramanian S, Kagan D, Hu C M J, et al. Micromachine-enabled capture and isolation of cancer cells in complex media. Angew Chem Int Ed, 2011, 50: 4161–4164
77 Orozco J, Cortes A, Cheng G, et al. Molecularly imprinted polymer-based catalytic micromotors for selective protein transport. J Am Chem Soc, 2013, 135: 5336–5339
78 Soler L, Magdanz V, Fomin V M, et al. Self-propelled micromotors for cleaning polluted water. ACS Nano, 2013, 7: 9611–9620
79 Kagan D, Campuzano S, Balasubramanian S, et al. Functionalized micromachines for selective and rapid isolation of nucleic acid targets from complex samples. Nano Lett, 2011, 11: 2083–2087
80 Campuzano S, Orozco J, Kagan D, et al. Bacterial isolation by lectin-modified microengines. Nano Lett, 2012, 12: 396–401
81 Kuralay F, Sattayasamitsathit S, Gao W, et al. Self-propelled carbohydrate-sensitive microtransporters with built-in boronic acid recognition for isolating sugars and cells. J Am Chem Soc, 2012, 134: 15217–15220
82 Moo J G, Pumera M. Chemical energy powered nano/micro/macromotors and the environment. Chem A Eur J, 2015, 21: 58–72
83 Soler L, Sanchez S. Catalytic nanomotors for environmental monitoring and water remediation. Nanoscale, 2014, 6: 7175–7182
84 Srivastava S K, Guix M, Schmidt O G. Wastewater mediated activation of micromotors for efficient water cleaning. Nano Lett, 2015, 16: 817–821
85 Vilela D, Parmar J, Zeng Y, et al. Graphene based microbots for toxic heavy metal removal and recovery from water. Nano Lett, 2016, 16: 2860–2866
86 Singh V V, Martin A, Kaufmann K, et al. Zirconia/graphene oxide hybrid micromotors for selective capture of nerve agents. Chem Mater, 2015, 27: 8162–8169
87 Wang H, Zhao G, Pumera M. Beyond platinum: Bubble-propelled micromotors based on Ag and MnO_2 catalysts. J Am Chem Soc, 2014, 136: 2719–2722
88 Zhao G, Ambrosi A, Pumera M. Clean room-free rapid fabrication of roll-up self-powered catalytic microengines. J Mater Chem A, 2014, 2: 1219–1223
89 Wang H, Moo J G, Pumera M. From nanomotors to micromotors: The influence of the size of an autonomous bubble-propelled device upon its motion. ACS Nano, 2016, 10: 5041–5050
90 Mou F, Pan D, Chen C, et al. Magnetically modulated pot-like $MnFe_2O_4$ micromotors: Nanoparticle assembly fabrication and their capability for direct oil removal. Adv Funct Mater, 2015, 25: 6173–6181
91 Giudicatti S, Marz S M, Soler L, et al. Photoactive rolled-up TiO_2 microtubes: Fabrication, characterization and applications. J Mater Chem C, 2014, 2: 5892–5901
92 Chen C, Mou F, Xu L, et al. Light-steered isotropic semiconductor micromotors. Adv Mater, 2016, doi: 10.1002/adma.201603374

Summary for “自驱动微纳米马达的设计原理与结构简化方法”

Design strategies and structure simplification methods of self-propelled micro-/nanomotors

KONG Lei, MOU FangZhi, JIANG YuZhou, LI XiaoFeng & GUAN JianGuo*

State Key Laboratory of Advanced Technology for Materials Synthesis and Processing, International School of Materials Science and Engineering, Wuhan University of Technology, Wuhan 430070, China
* Corresponding author, E-mail: guanjg@whut.edu.cn

Self-propelled micro-/nanomotors (MNMs), which are defined as micro-/nanodevices capable of converting various energy into autonomous motion, can be used to pick up, transport, and release various cargoes within a liquid medium. They have important potential applications, for example, in drug delivery, biosensors, protein and cell separation, microsurgeries and environment remediation. This review comprehensively introduces the design strategies and structures of self-propelled MNMs along with an outlook for their future development. It starts with the summary of the propulsion mechanisms of self-propelled MNMs of bubble recoiling and self-phoresis induced by the asymmetric release of products or heat. For bubble recoiling propulsion, the continuous momentum change is caused by a jet of bubbles, while for self-phoresis propulsion, the MNMs move in a local electric field, concentration gradient, surface tension gradient, or temperature gradient, etc. After systematically and in-depth understanding these propulsion mechanisms, it has been pointed out that the key to design self-propelled MNMs is to construct an asymmetric field across micro-/nanoparticles. Following this clue, the structures evolution and simplification methods of self-propelled MNMs are reviewed. Janus structures and multilayer-tubular structures, which are prepared through asymmetric modification process, electrochemical synthesis, template-assisted method, rolled-up nanotech, etc., have been firstly proposed to construct asymmetric fields across micro-/nanoparticles for their propulsion. However, the complicated structure and preparation process hinder the application of MNMs. Anisotropic single-component irregular particles, tubes and bowl-like MNMs, which are obtained by dry spinning method, “growing-bubble”-templated self-assembly, etc., have been subsequently achieved by utilizing their anomalous morphology and the nucleation preference of bubble molecules on different surfaces. This kind of MNMs show somewhat simple structure and can be easily fabricated, but the motion direction is still difficult to control because of the Brownian motion. Isotropic semiconducting MNMs have been recently developed by taking advantage of the limited light penetration depth in the isotropic photoresponsive particles, of which the motion is independent of the rotational Brownian motion. This suggests a remarkable breakthrough in design strategy of MNMs due to the simple isotropic structure of the motor and the controllability in both motion direction and speed by light. Besides the evolution of self-propelled MNMs from the complicated structure to the simplified one, some remarkable progresses have also been made on the motion control, functionalization, etc. For example, the speed and state of MNMs can so far be easily adjusted by the concentration of fuels, the intensity of external fields, etc. The direction can be controlled accurately by magnetic field, electric field, light, etc. Numerous complex tasks can also be performed effectively, such as protein separation, drug delivery, environmental detection and remediation, etc. Lastly, an outlook is also provided on the future development and main challenges of self-propelled MNMs. The future development of MNMs should be focused on improving energy conversion efficiency through optimization of structures, exploring new propulsion mechanisms and endowing MNMs with environmental responses for self-navigation, detection, and specific operations. In this way, MNMs will approach to the practical applications in biomedicine, environment treatment, microengineering, etc.

micro-/nanomotors, self-propulsion, asymmetric field, structure simplification

doi: 10.1360/N972016-00841